

# Semi-classical theory of collisional depolarization of spectral lines by atomic hydrogen. I: application to $p$ states of neutral atoms.

M. Derouich<sup>1</sup>, S. Sahal-Bréchet<sup>1</sup>, P. S. Barklem<sup>2</sup>, and B. J. O'Mara<sup>†3</sup>

<sup>1</sup> Observatoire de Paris-Meudon, LERMA FRE CNRS 2460, 5, Place Jules Janssen, F-92195 Meudon Cedex, France.

<sup>2</sup> Department of Astronomy and Space Physics, Uppsala University, Box 515, S 751 20 Uppsala, Sweden

<sup>3</sup> Department of Physics, The University of Queensland, St Lucia 4072, Australia  
e-mail: Moncef.Derouich@obspm.fr

Received 2002 / accepted 2003

**Abstract.** The present paper extends the method of Anstee, Barklem and O'Mara (Anstee 1992; Anstee & O'Mara 1991, 1995; Anstee, O'Mara & Ross 1997; Barklem 1998; Barklem & O'Mara 1997; Barklem, O'Mara & Ross 1998), developed during the 1990's for collisional line broadening by atomic hydrogen, to the depolarization of spectral lines of neutral atoms by collisions with atomic hydrogen. In the present paper, we will limit the calculations to  $p$  ( $l = 1$ ) atomic levels. The depolarization cross sections and depolarization rates are computed. In Table 2 cross sections as functions of the relative velocity and effective quantum number are given, allowing for the computation for any  $p$  atomic level. Our results are compared to quantum chemistry calculations where possible. The sensitivity of depolarization cross sections to regions of the potential is examined. We conclude that the accuracy obtained with our method ( $< 20\%$  for the depolarization rates) is promising for its extension to higher  $l$ -values for the interpretation of the "second solar spectrum". This will be the object of further papers.

**Key words.** Sun: atmosphere - atomic processes - line: formation, polarization - atomic data

## 1. Introduction

Observations of linear polarization at the limb of the Sun produce rich structures. This polarization spectrum (the so-called "second solar spectrum") is an entirely new spectrum to be explored and interpreted (Stenfo & Keller 1997). This polarization is due to scattering of the incident anisotropic solar radiation field. The radiative anisotropy is due to the structure of the semi-infinite or layer atmosphere in the vicinity of the surface, and is revealed by the center-to-limb darkening of the solar brightness.

In order to interpret quantitatively the Stokes parameters of the observed lines, a non-optically-thin and non-LTE model in the presence of a magnetic field has to be used. In fact, collision induced transitions between Zeeman sublevels can play a major role in depolarizing the levels (and thus the lines). Depolarizing collisions of the radiating and absorbing atoms with neutral hydrogen atoms of the medium have to be included in the statistical equilibrium equations. Very few depolarization rates have currently been computed, they have been obtained through sophisticated quantum chemistry methods which are accurate but cumbersome. It would be useful to develop methods capable of giving reasonable results for many levels rapidly. This is the object of the present work.

During the 1990's Anstee, Barklem and O'Mara (Anstee 1992; Anstee & O'Mara 1991, 1995; Anstee et al. 1997; Barklem 1998; Barklem & O'Mara 1997; Barklem et al. 1998) developed a new semi-classical theory, in order to obtain spectral line widths due to collisions with atomic hydrogen that were better than those obtained by the Van der Waals approximation. In this theory, which will be referred as ABO in the following, the scattering  $S$  matrix is obtained by solving semi-classical coupled differential equations. The hydrogen-atom interaction potential is derived from time-independent second-order perturbation theory without exchange, allowing the Lindholm-Foley average over  $m$  states (Brueckner 1971; O'Mara 1976) to be removed. Whereas the Van der Waals potential underestimates the broadening by typically a factor two or more, the ABO method gives rather good agreement ( $< 20\%$  for the spectral line widths) with the results obtained from quantum chemistry calculations. In addition, these authors used their ABO method by applying it to a selection of strong solar lines. The derived abundances are consistent with meteoritic ones.

In the present paper, we extend the ABO theory to the calculation of collisional depolarization rates which enter the statistical equilibrium equations for the polar-

ized atomic density matrix. This paper is focused on the method and is applied to  $p$  states of neutral atoms. We will present and compare our results with those recently obtained by quantum chemistry methods. We also compare the results to the depolarization rates calculated with the Van der Waals interaction. A discussion of our results is given, studying the region of the potential curves which play the major role in the variation of the depolarization cross sections. In conclusion, we show that our method, owing to the simplicity of the processes taken into account, is a useful alternative to the accurate but time consuming quantum chemistry method for obtaining most of the depolarization rates to better than 20 % accuracy. It should now be possible to rapidly obtain the large amount of data needed for the interpretation of the second solar spectrum, in particular for the heavy atoms that are inaccessible to present quantum chemistry calculations. An extension to  $d$  and  $f$  states is in progress. An extension to ions is in progress and this will be the subject of further papers.

## 2. Formulation of the problem

### 2.1. The statistical equilibrium equations (SEE) for polarization studies

The calculation of the Stokes parameters of a spectral line observed at the solar limb is a non-LTE (Local Thermodynamical Equilibrium) problem. It needs the solution of the coupling between the polarized radiative transfer and the statistical equilibrium equations (SEE) for the populations and coherences of the polarized atomic density matrix. In fact the atomic levels are only “aligned”, which means that the observed lines are globally linearly polarized. This linear polarization is due to anisotropic scattering of the incident solar radiation field which contributes to excitation of the atomic levels, the anisotropy being due to limb darkening, even at zero altitude above the limb.

Sahal-Bréchet (1977) developed the SEE for an “aligned” multilevel atom, i.e. for the Zeeman sublevels  $|\alpha JM_J\rangle$ . She took into account excitation by the anisotropic solar radiation field, deexcitation by spontaneous and induced emission, and excitation, deexcitation, polarization transfer and depolarization by isotropic collisions of the particles of the medium. She included the effect of a “strong” magnetic field (strong case of the Hanle effect) and thus coherences between Zeeman sublevels could be ignored. Only the populations of the Zeeman sublevels were taken into account.

She wrote these equations both in the dyadic basis  $|\alpha JM_J\rangle\langle\alpha' J' M'_J|$  built on the standard basis of the atomic states  $|\alpha JM_J\rangle$  and in the irreducible tensorial operator basis  ${}^{\alpha J \alpha' J'} T_q^k$ . The expansion of the  ${}^{\alpha J \alpha' J'} T_q^k$  over the dyadic basis is given by Fano & Racah (1959) (cf. also Messiah 1961; Fano 1963):

$${}^{\alpha J \alpha' J'} T_q^k = \sum_{M_J M'_J} (-1)^{J' - M'_J} \times |\alpha JM_J\rangle\langle\alpha' J' M'_J| \langle JJ' M_J - M'_J | k - q \rangle, \quad (1)$$

where  $\langle JJ' M_J - M'_J | k - q \rangle$  is a Clebsch-Gordan coefficient. She demonstrated the interest and power of this second basis, which is especially well adapted to problems with spherical and/or cylindrical symmetry processes. The equations are simplified, and the physics is extracted and highlighted. In particular, the odd  $k$ -terms can be eliminated from the SEE when the incident radiation field is anisotropic but unpolarized. In fact the natural radiation field transports  $k = 0$  (population) and  $k = 2$  (alignment) terms only. Orientation terms ( $k = 1$ ) vanish in the present astrophysical problem.

Sahal-Bréchet (1977) gave the general expressions for the various transition probabilities due to isotropic and anisotropic radiation and for isotropic collisions, i.e. expressions for population, orientation and alignment transfer between the levels, creation and destruction of population, orientation and alignment (depolarization rates in particular). At the same time, Omont (1977) developed a general theory of relaxation for a two-level atom. In addition he introduced coherences.

In fact, for isotropic processes, the coupling terms in the SEE implying transfer of coherence  $q \rightarrow q'$  are zero, and due to the isotropy of the collisions with hydrogen, the depolarization rates are  $q$ -independent. This is one of the advantages of the irreducible tensorial operator basis. Therefore, as we will consider isotropic collisions only in the following, it will be sufficient to calculate collisional cross sections between the sublevels, as for the no-coherence case (Sahal-Bréchet 1977), even if coherences play a role in the SEE. We recall that coherences can appear when the magnetic field is weak and not directed along the solar radius (Hanle effect). We also notice that in the present paper we are interested in hydrogen-atom collisions and not in electron or proton-ion collisions as in Sahal-Bréchet (1977). After integration of the cross sections over a Maxwell distribution of velocities and multiplying by the local hydrogen density, the depolarization rates obtained (and eventually polarization transfer rates between levels) can be used in the statistical equilibrium equations.

We focus on the collisional depolarization rates in the present paper. We will use both the dyadic and the irreducible tensorial operator bases. The latter one is in fact more convenient.

An important preliminary point to notice is the fact that the radiating atom can have a nuclear spin and thus hyperfine structure. The importance of the effect of the hyperfine structure on the Stokes parameters of the line studied was discussed for the example of the hydrogen coronal line  $\text{Ly}\alpha$  by Bommier & Sahal-Bréchet (1982). They showed that the SEE must be solved for the hyperfine levels when the inverse of the lifetime of the upper level is smaller than the hyperfine splitting, i.e. the hyperfine levels are separated. This arises from the Heisenberg uncertainty principle. On the contrary, when the hyperfine splitting is small compared to the inverse of the lifetime, the hyperfine levels are mixed and degenerate, the hyperfine structure can be ignored and the SEE can be solved

| F | $\Delta E_{HFS}(^2P_{3/2})$ | $\Delta E_{HFS}(^2S_{1/2})$ |
|---|-----------------------------|-----------------------------|
| 3 | 58.44                       | -                           |
| 2 | 34.32                       | 1772                        |
| 1 | 15.86                       | -                           |

**Table 1.** Values of the energy separation between the hyperfine levels  $F$  and  $F - 1$  for: Na in the ground state,  $3s \ ^2S_{1/2}$  (Ackermann 1966), and in the excited state  $3p \ ^2P_{3/2}$  (Gangrsky et al 1998). All energies are in MHz.

for the  $|\alpha J\rangle$  fine structure levels. This was the case for the hydrogen coronal line where the  $F$  levels are degenerate and the  $J$  levels are well separated.

In the second solar spectrum, where metallic lines are observed, the inverse of the lifetime (9.7 MHz for the Na D lines) (Gaupp et al 1982) is often small compared to the hyperfine splitting (if it exists) (cf. Table 1). Then the SEE must be solved for the  $|\alpha JF\rangle$  hyperfine levels (Bommier & Molodij 2002; Kerkeni & Bommier 2002) and collisional rates between the hyperfine sublevels must be calculated.

## 2.2. Dyadic basis for the depolarization rates

The depolarization arises from isotropic collisions between the Zeeman sublevels of a level  $|\alpha J\rangle$ : the collisions reestablish thermodynamical equilibrium between the sublevels and thus atomic polarization vanishes. We have to calculate (Sahal-Br echot 1977) for each sublevel  $|\alpha JM_J\rangle$  (or  $|\alpha JFM_F\rangle$  if there is an hyperfine structure):

$$D(\alpha JM_J, T) = \sum_{M'_J \neq M_J} \zeta(\alpha JM_J \rightarrow \alpha JM'_J, T) \quad (2)$$

where  $\zeta(\alpha JM_J \rightarrow \alpha JM'_J, T)$  is the collisional transition rate between the sublevels  $|\alpha JM_J\rangle \rightarrow |\alpha JM'_J\rangle$ . It can be written as a function of the local temperature  $T$  and the hydrogen perturber local density  $n_H$ :

$$\zeta(\alpha JM_J \rightarrow \alpha JM'_J, T) = n_H \int_0^\infty \sigma(\alpha JM_J \rightarrow \alpha JM'_J, v) \times v f(v) dv, \quad (3)$$

$f(v)$  being the distribution function for the atom-perturber relative velocity  $v$ , and  $\sigma(\alpha JM_J \rightarrow \alpha JM'_J, v)$  is the cross section. For the Maxwellian distribution,

$$f(v) = \sqrt{\frac{2}{\pi}} \left(\frac{\mu}{kT}\right)^{\frac{3}{2}} v^2 \exp\left(-\frac{\mu v^2}{2kT}\right), \quad (4)$$

where  $\mu$  is the reduced mass of the system.

The relaxation term for the density matrix (diagonal term of the system of SEE) due to collisions is given by:

$$\begin{aligned} \left(\frac{d^{\alpha J} \rho_{M_J M_J}}{dt}\right)_{coll} = & -D(\alpha JM_J, T) \alpha^J \rho_{M_J M_J} \quad (5) \\ & - \sum_{\alpha' J' \neq \alpha J} \sum_{M'_J} \zeta(\alpha JM_J \rightarrow \alpha' J' M'_J, T) \\ & \times \alpha^J \alpha'^{J'} \rho_{M_J M'_J} \end{aligned}$$

The terms added to the depolarization term  $D(\alpha JM_J, T)$  are the so-called quenching terms.

The dyadic basis is not suitable because the depolarization terms depend on the chosen dyadic basis. The  $\alpha^J \alpha'^{J'} T_q^k$  basis is well adapted because the depolarization terms do not depend on the basis and have a physical interpretation.

## 2.3. Basis of irreducible tensorial operators

In this basis, the SEE relaxation term in the non-coherence case ( $q = 0$ ) (Sahal-Br echot 1977; Omont 1977) becomes

$$\left(\frac{d^{\alpha J} \rho_0^k}{dt}\right)_{coll} = -D^k(\alpha J, T) \alpha^J \rho_0^k + \text{quenching term}, \quad (6)$$

where  $\alpha^J \rho_0^k$  is the multipole  $k$ -moment of the density matrix for the level  $|\alpha J\rangle$ . For isotropic collisions  $D^k(\alpha J, T)$  is characterized by  $(2J + 1)$  constants ( $0 \leq k \leq 2J$ ) and  $D^0(\alpha J, T)$  is called the destruction rate of population, which is zero for the no-quenching approximation.  $D^1(\alpha J, T)$  is the destruction rate of orientation (circular atomic polarization).  $D^2(\alpha J, T)$  is the destruction rate of alignment which is of interest in astrophysics (linear polarization), and the depolarization rate  $D^k(\alpha J, T)$  is given by:

$$D^k(\alpha J, T) = n_H \int_0^\infty \sigma^k(\alpha J, v) v f(v) dv \quad (7)$$

Using our present notation, formula (20) in Sahal-Br echot (1977) with  $k = k'$  can be written as:

$$\begin{aligned} \sigma^k(\alpha J, v) = & (2k + 1) \sum_{M'_J} \sum_{M_J \neq M'_J} (-1)^{2J-2M_J} \\ & \times \begin{pmatrix} J & k & J \\ -M_J & 0 & M_J \end{pmatrix}^2 \sigma(\alpha JM_J \rightarrow \alpha JM'_J, v) \\ & - (2k + 1) \sum_{M_J} \sum_{M'_J \neq M_J} (-1)^{2J-M_J-M'_J} \quad (8) \\ & \times \begin{pmatrix} J & k & J \\ -M_J & 0 & M_J \end{pmatrix} \begin{pmatrix} J & k & J \\ -M'_J & 0 & M'_J \end{pmatrix} \\ & \times \sigma(\alpha JM_J \rightarrow \alpha JM'_J, v) \end{aligned}$$

The expressions between parentheses denote  $3j$ -coefficients (Messiah 1961). After some calculations which are not detailed here, this equation can also be written as:

$$\begin{aligned} \sigma^k(\alpha J, v) = & \sigma(\alpha J, v) - (2k + 1) \sum_{M_J, M'_J} (-1)^{2J-M_J-M'_J} \\ & \times \begin{pmatrix} J & k & J \\ -M_J & 0 & M_J \end{pmatrix} \begin{pmatrix} J & k & J \\ -M'_J & 0 & M'_J \end{pmatrix} \quad (9) \\ & \times \sigma(\alpha JM_J \rightarrow \alpha JM'_J, v). \end{aligned}$$

Where  $\sigma(\alpha J, v)$  is the elastic cross section for the level  $|\alpha J\rangle$  and the relative velocity  $v$ :

$$\sigma(\alpha J, v) = \sum_{M'_J} \sigma(\alpha JM_J \rightarrow \alpha JM'_J, v) \quad (10)$$

This cross section can also be written as an average over the initial states  $M_J$  as usual:

$$\sigma(\alpha J, v) = \frac{1}{2J+1} \sum_{M_J, M'_J} \sigma(\alpha J M_J \rightarrow \alpha J M'_J, v) \quad (11)$$

where the angular average over all the directions of the collisions is not necessary here because the averaging over  $M'_J$  is equivalent to the angular average over the directions of the collision. This property will be used in Sect. 6, first line in equation (41).

Since the depolarization cross section  $\sigma^k(\alpha J, v)$  can be written as a linear combination of the  $\sigma(\alpha J M_J \rightarrow \alpha J M'_J, v)$ , the depolarization rate  $D^k(\alpha J, v)$  is a linear combination of the collisional rates between the Zeeman sublevels  $\zeta(\alpha J M \rightarrow \alpha J M')$  (Sahal-Bréchet 1977). In particular we have (Sahal-Bréchet 1977), for  $J = 1$ :

$$D^1(\alpha 1) = \zeta(10 \rightarrow 1 \pm 1) + 2\zeta(1 \mp 1 \rightarrow 1 \pm 1)$$

$$D^2(\alpha 1) = 3\zeta(10 \rightarrow 1 \pm 1),$$

and for  $J = 3/2$  (Gordeyev et al 1969; Roueff & Suzor 1974):

$$D^1(\alpha \frac{3}{2}) = \frac{1}{5} \zeta(\frac{3}{2} \frac{-1}{2} \rightarrow \frac{3}{2} \frac{1}{2}) + \frac{2}{5} \zeta(\frac{3}{2} \frac{3}{2} \rightarrow \frac{3}{2} \frac{1}{2}) \\ + \frac{8}{5} \zeta(\frac{3}{2} \frac{-3}{2} \rightarrow \frac{3}{2} \frac{1}{2}) + \frac{9}{5} \zeta(\frac{3}{2} \frac{-3}{2} \rightarrow \frac{3}{2} \frac{3}{2})$$

$$D^2(\alpha \frac{3}{2}) = 2\zeta(\frac{3}{2} \frac{3}{2} \rightarrow \frac{3}{2} \frac{1}{2}) + 2\zeta(\frac{3}{2} \frac{-1}{2} \rightarrow \frac{3}{2} \frac{1}{2}) \\ + 2\zeta(\frac{3}{2} \frac{-3}{2} \rightarrow \frac{3}{2} \frac{1}{2})$$

$$D^3(\alpha \frac{3}{2}) = \frac{9}{5} \zeta(\frac{3}{2} \frac{-1}{2} \rightarrow \frac{3}{2} \frac{1}{2}) + \frac{8}{5} \zeta(\frac{3}{2} \frac{3}{2} \rightarrow \frac{3}{2} \frac{1}{2}) \\ + \frac{2}{5} \zeta(\frac{3}{2} \frac{-3}{2} \rightarrow \frac{3}{2} \frac{1}{2}) + \frac{1}{5} \zeta(\frac{3}{2} \frac{-3}{2} \rightarrow \frac{3}{2} \frac{3}{2})$$

### 3. Calculation of the cross sections

We will use a semi-classical treatment for the collision: we will assume that the hydrogen perturbing atom moves along a straight path, unperturbed by the collision process and characterized by an impact-parameter  $b$ .

In the dyadic basis  $|\alpha J M_J\rangle\langle\alpha' J' M'_J|$  (or  $|\alpha J F M_F\rangle\langle\alpha' J' F' M'_F|$  if there is an hyperfine structure), the cross section follows from an integration over the impact-parameter  $b$  and averaging the transition probability  $P(\alpha J M_J \rightarrow \alpha J M'_J, \mathbf{b}, \mathbf{v})$  over all the collision directions:

$$\sigma(\alpha J M_J \rightarrow \alpha J M'_J, v) = \int_0^\infty 2\pi b db \left( \frac{1}{8\pi^2} \right. \\ \left. \times \oint P(\alpha J M_J \rightarrow \alpha J M'_J, \mathbf{b}, \mathbf{v}) d\Omega \right) \quad (12)$$

and then the collisional transition rate is given by equation (3). The transition probability can be written in terms of the  $S$ -matrix elements,

$$P(\alpha J M_J \rightarrow \alpha J M'_J, \mathbf{b}, \mathbf{v}) = \\ |\langle\alpha J M_J | I - S(\mathbf{b}, \mathbf{v}) | \alpha J M'_J \rangle|^2 \quad (13)$$

where  $I$  is the unit matrix and  $T = I - S$  is the so-called transition matrix.

#### 3.1. Calculation of the $S$ -matrix

The Hamiltonian of the system atom-perturber can be written as:

$$H = H_A + H_P + V, \quad (14)$$

where  $H_A$  is the atomic Hamiltonian,  $H_P$  that of the perturber and  $V$  is the interaction energy.  $H_A$  can be written as:

$$H_A = H_0 + H_{FS} + H_{HFS}, \quad (15)$$

where  $H_0$  contains the electrostatic part,  $H_{FS}$  the fine structure and  $H_{HFS}$  the hyperfine structure if it exists.

It can be shown that the hyperfine splitting  $\Delta E_{HFS}$  is always small when compared to  $V$  and thus  $J$  and  $I$  (the nuclear spin) can be decoupled during the collision process. This arises from the Heisenberg uncertainty principle: if  $\tau$  is a typical collision time, one can ignore the hyperfine structure if

$$\tau \Delta E_{HFS} \ll 1, \quad (16)$$

where  $\tau \sim \frac{b}{v}$ ,  $b$  being a typical impact-parameter (of the order of  $10a_0$ ,  $a_0$  being the Bohr radius) and  $v \sim 4.8 \times 10^{-3}$  a.u. for a temperature of about 5000 K so that  $\tau \sim 2.08 \times 10^3$  a.u.. In the case of the Na atom the nuclear spin is  $I = 3/2$ , which yields two hyperfine levels in the ground state  $3s^2 S_{1/2}$ ,  $F = 1$  and  $F = 2$ . For the excited  $3p^2 P_{3/2}$  state there are four hyperfine levels:  $F = 0$ ,  $F = 1$ ,  $F = 2$  and  $F = 3$ . The energy differences between these levels are given in Table 1. In the case of the ground state  $3s^2 S_{1/2}$ ,  $\Delta E_{HFS} \simeq 2.694 \times 10^{-7}$  a.u. (1772 MHz) (Ackermann 1966) and then  $\tau \Delta E_{HFS} \simeq 5.6 \times 10^{-4} \ll 1$ . For the excited level the most important hyperfine splitting is, of course, between the levels  $F = 0$  and  $F = 3$  where  $\Delta E_{HFS} \simeq 1.653 \times 10^{-8}$  a.u. (108.72 MHz) (Gangrsky et al 1998) and then  $\tau \Delta E_{HFS} \simeq 3.4 \times 10^{-5} \ll 1$ .

The hyperfine splitting can always be ignored in the treatment of the collision under these conditions. We have  $\mathbf{F} = \mathbf{I} + \mathbf{J}$  and  $M_F = M_I + M_J$ , and

$$|\alpha J F M_F\rangle = \sum_{M_I, M_J} \langle I J M_I M_J | F M_F \rangle |J M_J\rangle |I M_I\rangle, \quad (17)$$

where  $\langle I J M_I M_J | F M_F \rangle$  is a Clebsch-Gordan coefficient. Then the matrix element

$$\langle \alpha J F M_F | S | \alpha' J' F' M'_F \rangle = \sum_{M_I, M_J, M'_I, M'_J} \langle I J M_I M_J | F M_F \rangle \\ \times \langle I J' M'_I M'_J | F' M'_F \rangle \langle \alpha J M_J | \langle I M_I | S | I M'_I \rangle | \alpha' J' M'_J \rangle. \quad (18)$$

If the hyperfine structure can be neglected during the collision, the  $S$ -matrix is diagonal in  $I$  and its elements do not depend on  $M_I$  ( $I$  is conserved). Thus  $M'_I = M_I$  and

$$\langle \alpha J F M_F | S | \alpha' J' F' M'_F \rangle = \sum_{M_I, M_J, M'_J} \langle I J M_I M_J | F M_F \rangle \\ \times \langle I J' M_I M'_J | F' M'_F \rangle \langle \alpha J M_J | S | \alpha' J' M'_J \rangle \quad (19)$$

This relation holds for each impact-parameter and each relative velocity.

We recall the relation between Clebsch-Gordan coefficients and  $3j$ -coefficients:

$$\langle j_1 j_2 m_1 m_2 | j m \rangle = \sqrt{2j+1} (-1)^{j_1-j_2+m} \begin{pmatrix} j_1 & j_2 & j \\ m_1 & m_2 & -m \end{pmatrix}$$

We use the convention of Messiah (1961) for the phase factors.

### 3.2. Calculation of the $S$ -matrix elements between fine sublevels

The fine structure splitting can generally be neglected during the collision problem at the temperature of interest in the second solar spectrum ( $\sim 5000K$ ). The validity of the condition is the same as above, except that the fine structure splitting is larger than the hyperfine splitting. For example in the case of the Na atom, at  $5000K$ ,  $\Delta E_{FS} \simeq 0.78 \times 10^{-4}$  a.u. and  $\tau \simeq 2.08 \times 10^3$  a.u. and so  $\tau \Delta E_{FS} \simeq 0.16 < 1$ . This has been discussed in earlier papers focussed on collisional line broadening, see for example Roueff (1974) and related papers. She showed that the fine structure splitting is of importance at low temperatures (200-500 K) for the sodium  $D$  lines and negligible at higher temperatures for line broadening studies (500 K and higher). The  $D_1$  and  $D_2$  lines have in fact the same collisional width for hydrogen perturbors at solar temperatures.

If the fine structure is neglected, where  $\mathbf{J} = \mathbf{S} + \mathbf{L}$ , and  $M_J = M_S + m_l$ , we have:

$$\langle \alpha l J M_J | S | \alpha' l' J' M'_J \rangle = \sum_{M_S, m_l, m'_l} \langle S l M_S m_l | J M_J \rangle \quad (20)$$

$$\times \langle S l' M_S m'_l | J' M'_J \rangle \langle \alpha m_l | S | \alpha' l' m'_l \rangle,$$

cf. equation (19).

However, we notice that the parallelism between line broadening and depolarization cross sections must be used carefully in the peculiar following case. Depolarization of hyperfine components of spherically symmetric  $J = J' = 1/2$  levels (ground state of sodium for instance), needs the matrix elements  $M_J = \pm \frac{1}{2} \rightarrow M'_J = \pm \frac{1}{2}$ . If the fine structure is neglected, they are zero and the depolarization and polarization transfer rates of the hyperfine components of the ground states are zero. Kerkeni et al (2000) calculated the hyperfine collisional depolarization rates for the ground state of sodium with a quantum chemistry method which takes into account the fine structure splitting during the interaction processes. They showed that these rates are of the same order of magnitude as those of upper levels for which the fine structure splitting plays a minor role in the collisional processes. In fact this remark does not concern  $l \geq 1$  states and is very specific. However, we consider that it is important to mention it.

## 4. The model of Anstee, Barklem and O'Mara (ABO)

The present semi-classical model used for the depolarization is the same one as that already developed for line broadening theory applications in the 1990's by Anstee, Barklem and O'Mara (Anstee 1992; Anstee & O'Mara 1991, 1995; Anstee et al. 1997; Barklem 1998; Barklem & O'Mara 1997, Barklem et al. 1998).

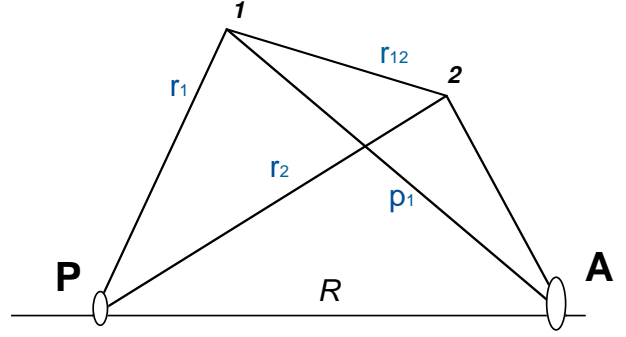


**Fig. 1.** The perturbed atom core is located at A and the hydrogen perturbing core (a proton) at P. Their valence electrons are denoted by 1 and 2 respectively.

The theory is described in these papers, and thus only a brief review is presented in the following:

1. The model is of semi-classical nature, the internal states of the two atoms are treated within the framework of quantum mechanics and the collision is modelled with the straight path classical approximation: it is assumed that the interparticle interaction is too weak to deflect the perturbed particle from the straight classical path.

2. The interaction energy between the two atoms is smaller than the energy eigenvalues of the isolated atoms, so that the Rayleigh-Schrödinger perturbation theory can be used for obtaining perturbed eigenvalues. Ionic and exchange interactions are neglected. The hyperfine and fine structure interactions are also neglected.

3. Time-independent perturbation theory is applied to second order. It is assumed that the energy denominator in the second order term can be replaced by a suitable average energy  $E_p$ . This is the Unsöld approximation (Unsöld 1927; Unsöld 1955). The value  $E_p = -4/9$ , in atomic units, is adopted. This approximation works when the energy level separations of the perturbed atom are small compared with those of hydrogen. For neutral atoms this condition is generally satisfied. This is particularly valid when considering interactions with hydrogen in the ground state, like in this work, which is well separated from any other levels (Anstee & O'Mara 1991).

4. Unperturbed atomic eigenfunctions are used. The Coulomb approximation with quantum defect is used.

## 5. Treatment of the collision

Each collision is characterized by an impact-parameter vector  $\mathbf{b}$  and a relative velocity vector  $\mathbf{v}$ . Since the hyperfine and fine structure interactions are neglected, equation (14) becomes:

$$H = H_0 + H_P + V \quad (21)$$

where  $V$  is the interaction energy which is assumed to be totally electrostatic. Only  $V$  depends on time. In the coordinate system of Fig. 1,  $V$  is given, in atomic units, by (Anstee & O'Mara 1991):

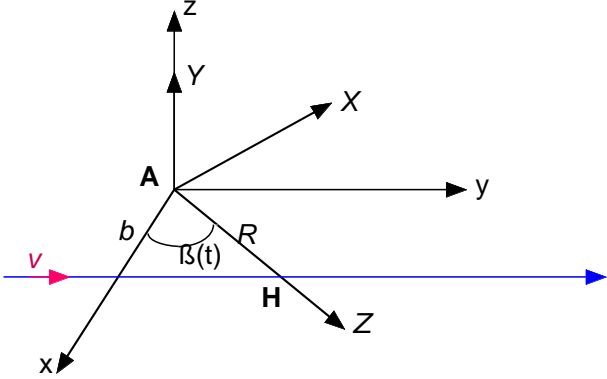


**Fig. 2.** Trajectory of the perturber (H) in the two reference frames.  $R$  is the interatomic separation,  $R = \sqrt{b^2 + v^2 t^2}$ .  $Axyz$  and  $AXYZ$  are the atomic and rotating frames.

$$V = \frac{1}{R} + \frac{1}{r_{12}} - \frac{1}{r_2} - \frac{1}{p_1} \quad (22)$$

and atomic units are used hereafter.

Since the hydrogen perturber remains in its ground state  $1s$  during the collision, the wave function  $|\psi\rangle$  of the system (atom+perturber), is the product of the wave functions  $|\psi\rangle_{(A)}$  of the perturbed atom and that of hydrogen in its ground state  $|100\rangle_{(H)}$ :

$$|\psi\rangle = |\psi\rangle_{(A)}|100\rangle_{(H)}. \quad (23)$$

The eigenenergy of the hydrogen perturber in its ground state is denoted by  $E_H^0$ . Following Anstee & O'Mara (1991), we use second-order time-independent perturbation theory for the eigenenergy of the system.

We also use the unperturbed atomic wave functions defined by:

$$H_0|nlm_l\rangle = E_{nlm_l}^0|nlm_l\rangle; |\psi\rangle_{(A)} = |nlm_l\rangle. \quad (24)$$

They form a complete set of eigenfunctions  $|nlm_l\rangle$  and eigenvalues  $E_{nlm_l}^0$ . The perturbed eigenvalues of the system of Hamiltonian  $H$  can be written as:

$$E_i = E_i^0 + \langle i|V|i\rangle + \sum_{j \neq i} \frac{\langle i|V|j\rangle\langle j|V|i\rangle}{E_i^0 - E_j^0}, \quad (25)$$

the summation being over all product states  $|j\rangle = |\psi\rangle_{(A)}|\psi\rangle_{(H)}$  except  $|i\rangle = |nlm_l\rangle_{(A)}|100\rangle_{(H)}$ , and where  $E_i^0 = E_{nlm_l}^0 + E_H^0$ .

Quenching is neglected and thus we consider only the subspace  $nl$  ( $2l+1$  states) and we denote the product state of the two separated atom at  $R = \infty$  by  $|M_l\rangle$  (Anstee & O'Mara 1991),

$$|M_l\rangle = |i\rangle = |nlm_l\rangle_{(A)}|100\rangle_{(H)}. \quad (26)$$

We introduce an effective potential  $V_{eff}$ , the diagonal elements of which are defined as

$$\langle M_l|V_{eff}|M_l\rangle = E_{M_l} - E_{M_l}^0 \quad (27)$$

The evaluation of the second order contribution to the above expression (25) is very difficult because it requires a summation over the complete set of eigenstates of the two isolated atoms. However, the expression can be greatly simplified by using the Unsöld approximation, i.e. by replacing  $E_i^0 - E_j^0$  by the constant value  $E_p$ . With this approximation, the expression for  $V_{eff}$  becomes

$$\begin{aligned} \langle M_l|V_{eff}|M_l\rangle &= \langle M_l|V|M_l\rangle - \frac{1}{E_p}(\langle M_l|V|M_l\rangle)^2 \\ &+ \frac{1}{E_p}\langle M_l|V^2|M_l\rangle, \end{aligned} \quad (28)$$

where  $\langle M_l|V_{eff}|M_l\rangle$  is the so-called Rayleigh-Schrödinger-Unsöld (RSU) potential which is used throughout the ABO model. Then, for computing the RSU potential, explicit expressions for the wave functions are needed.

The perturbed atom is modelled as a single valence electron outside a spherical ionic core. The chosen radial functions are of Coulomb type (Seaton 1958). The quantum defect and thus the effective quantum number  $n^* = [2(E_\infty - E_{nl})]^{-1/2}$  is a fundamental ingredient of the calculation of the interaction potential used in the ABO model. We refer to the ABO papers for more details concerning the interaction potential.

The  $S$ -matrix requires the time-dependent Schrödinger equation to be solved, i.e.

$$(H_0 + H_P + V_{eff})|\psi(t)\rangle = i\frac{d|\psi(t)\rangle}{dt} \quad (29)$$

where the interaction potential  $V$  is now replaced by  $V_{eff}$ . The  $S$ -scattering matrix is defined by:

$$S = U(+\infty, -\infty) \quad (30)$$

where  $U(+\infty, -\infty)$  is the evolution operator in the interaction representation, where

$$\tilde{\psi}(t+s) = U^\dagger(t+s, t)\psi(t) = e^{i(H_0+H_P)s}\psi(t), \quad (31)$$

is the corresponding wave function. The wave function is expressed in terms of the basis formed by the eigenvectors  $|M_l\rangle$  of  $(H_0 + H_P)$  given by (26) so that:

$$|\psi(t)\rangle = \sum_{M_l} a_{M_l}(t)e^{-iE_{M_l}^0 t}|M_l\rangle; \quad (32)$$

$$|\tilde{\psi}(t)\rangle = \sum_{M_l} a_{M_l}(t)|M_l\rangle$$

and we obtain a system of  $(2l+1)$  coupled linear differential equations of first order:

$$i\frac{\partial a_{M_i}(t)}{\partial t} = \sum_{M_k=-l}^l a_{M_k}(t)\langle M_l|V_{eff}|M_k\rangle. \quad (33)$$

We have to solve this system for the initial conditions:

$$a_{M_l}(-\infty) = \delta(M_i, M_l), \quad (34)$$

where  $\delta$  is the Kronecker symbol and

$$\langle M_l|S|M_i\rangle = \langle M_i|S|M_l\rangle = a_{M_i}(+\infty). \quad (35)$$

Thus the system has to be solved  $(2l+1)$  times for obtaining all the elements of the  $S$ -matrix for the  $(nl)$  subspace.

For the calculations, two frames of reference are used. The first one is the atomic frame in which the perturbed atom is stationary at the origin, the quantization axis is taken as perpendicular to the collision plane  $(\mathbf{b}, \mathbf{v})$  and the second one is the rotating or molecular frame in which the interatomic axis is taken as the quantization axis. These reference frames are shown in Fig. 2. This choice of frames gives the simplest relationship between states quantized relative to the atomic and the rotating frames respectively (Roueff 1974).

The interaction potential  $V$  has a cylindrical symmetry about the internuclear axis  $(OZ)$  and so  $V_{eff}$  is diagonal in the rotating frame.

A transformation of the angular momentum states from the atomic basis to the rotating frame is achieved by using the rotations matrices (Messiah 1961). The Euler angles are given by  $(\beta, \frac{\pi}{2}, \frac{\pi}{2})$  and equation (33) becomes

$$i\frac{\partial a_{M_i}(t)}{\partial t} = \sum_{M_k M'_k} \mathcal{D}_{M_l M'_k}^{(l)} \mathcal{D}_{M_l M'_k}^{\dagger(l)} a_{M_k}(t) \langle M_l|V_{eff}|M_l\rangle \quad (36)$$

when  $\mathcal{D}$  is the rotation operator.

For a given quantum number  $l$  we obtain  $(2l+1)$  coupled differential equations. These coupled equations must be solved for obtaining the  $(2l+1)^2$   $S$ -matrix elements.

The interaction matrix is Hermitian and the  $S$ -matrix is unitary and symmetric. If the quantization axis is perpendicular to the collision plane the selection rules are:  $\Delta m_l = \pm 2, \pm 4, \dots$ . This rule will disappear when we take an average over all possible orientations of the collision plane, since the collisions are isotropic.

## 6. Depolarization calculations for $l = 1$

Let us consider collisions between an atom in an  $l = 1$  state and hydrogen in its ground state  $1s$ . The state of the system during the collision becomes explicitly:

$$|\psi(t)\rangle = a_1(t)|11\rangle|00\rangle e^{-iE_1^0 t} + a_0(t)|10\rangle|00\rangle e^{-iE_0^0 t} + a_{-1}(t)|1-1\rangle|00\rangle e^{-iE_{-1}^0 t} \quad (37)$$

and the coupled differential equations become (Anstee & O'Mara 1991):

$$\begin{aligned} i\frac{\partial a_1(t)}{\partial t} &= a_1(t)V_+ + e^{2i\beta} a_{-1}(t)V_- \\ i\frac{\partial a_0(t)}{\partial t} &= a_0(t)\langle 1|V_{eff}|1\rangle \end{aligned} \quad (38)$$

$$i\frac{\partial a_{-1}(t)}{\partial t} = a_{-1}(t)V_+ + e^{-2i\beta} a_1(t)V_-$$

where:

$$V_{\pm} = \frac{1}{2}(\langle 1|V_{eff}|1\rangle \pm \langle 0|V_{eff}|0\rangle). \quad (39)$$

The equations are integrated with a Runge-Kutta-Merson routine and then we obtain the transition matrix elements in the  $|\alpha l m_l\rangle$  basis for a given velocity and impact-parameter.

We recall that we need, for depolarization calculations, the  $T$ -matrix elements in the  $|\alpha J M_J\rangle$  basis. Since the spin is neglected, the  $S$ -matrix is diagonal in  $S$  and its elements do not depend on  $M_S$ . Following equation (20) we obtain:

$$\begin{aligned} \langle \alpha J M_J|T|\alpha J M'_J\rangle &= \sum_{m_l, m'_l, M_S} (-1)^{2S-2l+M_J+M'_J} (2J+1) \\ &\times \begin{pmatrix} S & l & J \\ M_S & m_l & -M_J \end{pmatrix} \\ &\times \begin{pmatrix} S & l & J \\ M_S & m'_l & -M'_J \end{pmatrix} \langle \alpha l m_l|T|\alpha l m'_l\rangle \end{aligned} \quad (40)$$

The matrix elements  $\langle \alpha J M_J|T|\alpha J M'_J\rangle$  are obtained in a basis where the quantization axis is perpendicular to the collision plane. We have now to perform an average of the transitions probabilities over all possible orientations since collisions are isotropic. This angular average is denoted by  $\langle \rangle_{av}$ .

Using formula (16) by Sahal-Bréchet (1973), it can be shown that, in the irreducible tensorial operator basis, the angular average of the depolarization transition probability is given by:

$$\begin{aligned} \langle P^k(\alpha J, b, v)\rangle_{av} &= \frac{1}{2J+1} \sum_{\mu, \mu'} |\langle \alpha J \mu|T|\alpha J \mu'\rangle|^2 \\ &- \sum_{\mu, \mu', \nu, \nu'} \langle \alpha J \mu|T|\alpha J \mu'\rangle \langle \alpha J \nu|T|\alpha J \nu'\rangle^* \\ &\times \sum_{\chi} (-1)^{2J+k+\mu-\mu'} \begin{pmatrix} J & J & k \\ -\nu' & \mu' & \chi \end{pmatrix} \begin{pmatrix} J & J & k \\ \nu & -\mu & -\chi \end{pmatrix} \end{aligned} \quad (41)$$

Owing to the selection rules on the  $3j$ -coefficients, the summation over  $\chi$  is reduced to a single term, since  $\chi = -(\mu' - \nu') = -(\mu - \nu)$ .

The depolarization cross section may then be computed from:

$$\sigma^k(\alpha J, v) = 2\pi \int_0^\infty \langle P^k(\alpha J, b, v)\rangle_{av} b db \quad (42)$$

At small impact-parameters, the  $\langle P^k(\alpha J, b, v)\rangle_{av}$  values become highly oscillatory, and it is impractical to integrate

numerically. In addition, at these separations the perturbation theory breaks down and the calculated RSU potentials become invalid. Thus, an impact-parameter cutoff is used (Anstee & O'Mara 1991):

$$\sigma^k(\alpha J, v) \simeq \pi b_0^2 + 2\pi \int_{b_0}^{\infty} \langle P^k(\alpha J, b, v) \rangle_{av} b db \quad (43)$$

Integration over the velocity distribution for a temperature  $T$  can be performed to obtain the depolarization rate which is given by:

$$D^k(\alpha J, T) \simeq n_H \int_0^{\infty} v f(v) dv \left( \pi b_0^2 + 2\pi \int_{b_0}^{\infty} \langle P^k(\alpha J, b, v) \rangle_{av} b db \right) \quad (44)$$

where  $b_0$  is the cutoff impact-parameter and here  $b_0 = 3a_0$  as in Anstee & O'Mara (1991) (see Sect. 8).

## 7. Results

### 7.1. Our results for $^1P_1$ and $^2P_{3/2}$ levels

The perturbed atom is modelled as a single valence electron outside a spherical ionic core. If the energy of the state  $|\alpha l\rangle$  of the valence electron is denoted by  $E_{\alpha l}$  and the binding energy of the ground state by  $E_{\infty}$ , the binding energy of the level  $|\alpha l\rangle$  is  $(E_{\infty} - E_{\alpha l})$  and is related to the effective principal quantum number by  $n^* = [2(E_{\infty} - E_{nl})]^{-1/2}$ .

For example: consider the case of the neutral calcium line  $4227\text{\AA}$  (transition  $4s^2 - 4s4p$ ). The energy of the  $4p$  level and the binding energy are  $\simeq 0.1077\text{a.u.}$  ( $\sim 23652\text{ cm}^{-1}$ ) and  $\simeq 0.2245\text{a.u.}$  ( $49305.72\text{ cm}^{-1}$ ) respectively (Wiese et al 1969). Hence the effective principal quantum number is  $n^* \simeq 2.077$ .

Note that if the parent configuration of the level is not the same as that of the ground state, this should be accounted for by using the appropriate series limit for the excited parent configuration instead of the ground state binding energy. A particular example was explained in detail by Barklem, Anstee & O'Mara (1998) (see also Barklem, Piskunov & O'Mara 2000). As in Anstee & O'Mara (1991), we can calculate the cross sections as a function of  $n^*$ . Table 2 gives  $\sigma^k(\alpha 1, v)$  and  $\sigma^k(\alpha \frac{3}{2}, v)$  as a function of  $n^*$  for a typical relative velocity  $v = 10\text{ km s}^{-1}$ .

We thus can obtain the depolarization cross section for any level of any atom by interpolation of the values given in Table 2 for the appropriate  $n^*$  value for the state of interest. We notice that the dependence of cross sections on velocity is very close to

$$\sigma^k(\alpha J, v) = \sigma^k(\alpha J, v_0) \left(\frac{v}{v_0}\right)^{-\lambda^k(\alpha J)}, \quad (45)$$

where  $v_0$  is the velocity at which the cross section is known ( $10\text{ km s}^{-1}$ ). Table 3 shows the so-called velocity exponent  $\lambda^k(\alpha J)$  (Anstee & O'Mara 1991). In order to obtain the

| $n^*$ | $\sigma^1(\alpha 1)$ | $\sigma^2(\alpha 1)$ | $\sigma^1(\alpha \frac{3}{2})$ | $\sigma^2(\alpha \frac{3}{2})$ | $\sigma^3(\alpha \frac{3}{2})$ |
|-------|----------------------|----------------------|--------------------------------|--------------------------------|--------------------------------|
| 1.5   | 203                  | 192                  | 79                             | 141                            | 134                            |
| 1.6   | 233                  | 228                  | 90                             | 165                            | 157                            |
| 1.7   | 276                  | 258                  | 100                            | 187                            | 176                            |
| 1.8   | 323                  | 301                  | 114                            | 217                            | 203                            |
| 1.9   | 377                  | 349                  | 130                            | 252                            | 233                            |
| 2     | 438                  | 405                  | 147                            | 290                            | 268                            |
| 2.1   | 507                  | 466                  | 167                            | 334                            | 307                            |
| 2.2   | 581                  | 533                  | 189                            | 381                            | 349                            |
| 2.3   | 663                  | 605                  | 212                            | 432                            | 393                            |
| 2.4   | 751                  | 683                  | 237                            | 487                            | 442                            |
| 2.5   | 849                  | 769                  | 266                            | 549                            | 496                            |
| 2.6   | 949                  | 869                  | 295                            | 616                            | 562                            |
| 2.7   | 1058                 | 970                  | 327                            | 685                            | 627                            |
| 2.8   | 1180                 | 1075                 | 362                            | 761                            | 691                            |
| 2.9   | 1299                 | 1176                 | 396                            | 835                            | 753                            |
| 3     | 1423                 | 1282                 | 431                            | 911                            | 817                            |

**Table 2.** Variation of the depolarization cross section, for a relative velocity of  $10\text{ km s}^{-1}$ , with effective principal quantum number. Cross sections are in atomic units.

| $n^*$ | $\lambda^1(\alpha 1)$ | $\lambda^2(\alpha 1)$ | $\lambda^1(\alpha \frac{3}{2})$ | $\lambda^2(\alpha \frac{3}{2})$ | $\lambda^3(\alpha \frac{3}{2})$ |
|-------|-----------------------|-----------------------|---------------------------------|---------------------------------|---------------------------------|
| 1.5   | 0.269                 | 0.256                 | 0.201                           | 0.246                           | 0.240                           |
| 1.6   | 0.270                 | 0.257                 | 0.207                           | 0.246                           | 0.234                           |
| 1.7   | 0.265                 | 0.247                 | 0.211                           | 0.244                           | 0.235                           |
| 1.8   | 0.259                 | 0.249                 | 0.213                           | 0.242                           | 0.240                           |
| 1.9   | 0.256                 | 0.242                 | 0.215                           | 0.240                           | 0.234                           |
| 2     | 0.251                 | 0.235                 | 0.216                           | 0.237                           | 0.235                           |
| 2.1   | 0.253                 | 0.237                 | 0.220                           | 0.235                           | 0.218                           |
| 2.2   | 0.248                 | 0.235                 | 0.219                           | 0.232                           | 0.223                           |
| 2.3   | 0.246                 | 0.235                 | 0.221                           | 0.231                           | 0.221                           |
| 2.4   | 0.242                 | 0.231                 | 0.220                           | 0.230                           | 0.225                           |
| 2.5   | 0.240                 | 0.224                 | 0.221                           | 0.228                           | 0.224                           |
| 2.6   | 0.242                 | 0.227                 | 0.223                           | 0.228                           | 0.220                           |
| 2.7   | 0.241                 | 0.223                 | 0.224                           | 0.228                           | 0.226                           |
| 2.8   | 0.244                 | 0.226                 | 0.228                           | 0.230                           | 0.223                           |
| 2.9   | 0.249                 | 0.223                 | 0.221                           | 0.230                           | 0.208                           |
| 3     | 0.243                 | 0.229                 | 0.229                           | 0.2208                          | 0.225                           |

**Table 3.** Velocity exponents  $\lambda^k(\alpha J)$  corresponding to the cross sections of Table 2.

depolarization cross section for any velocity  $v$  from Tables 2 and 3 equation (45) can be used.

Figures 3 and 4 display the depolarization cross sections (computed directly) and the corresponding depolarization rates for the CaI  $4p\ ^1P_1$  ( $n^* \simeq 2.077$ ), MgI  $3p\ ^1P_1$  ( $n^* \simeq 2.030$ ) and the NaI  $3p\ ^2P_{3/2}$  ( $n^* \simeq 2.117$ ) states.

To obtain the depolarization rates we must integrate over the Maxwell distribution of velocities. Using equation (44), it can be shown that for a mean velocity  $\bar{v} = \sqrt{\frac{8kT}{\pi\mu}}$ , the depolarization rates can be expressed as (Anstee & O'Mara 1991)



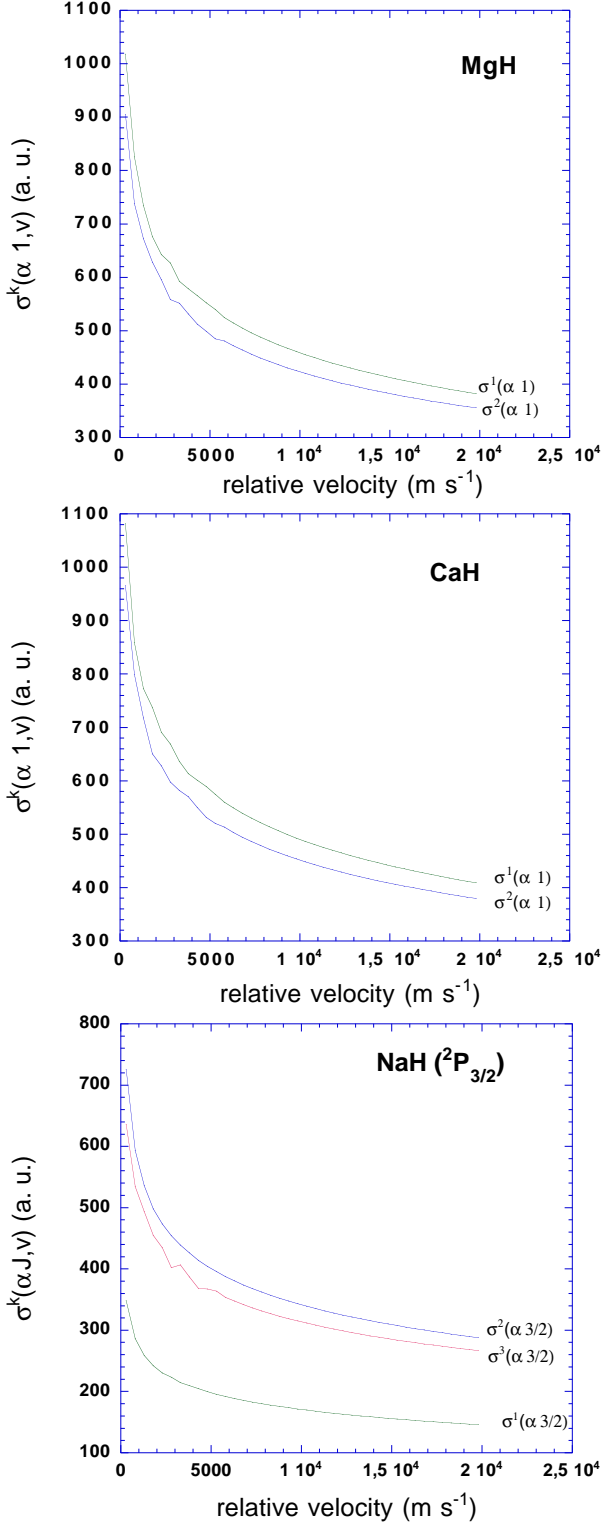


**Fig. 3.** Depolarization cross sections as a function of relative velocity.

$$D^k(\alpha, J, T) = \left(\frac{4}{\pi}\right)^{\frac{1}{2}} \lambda^k(\alpha, J) \Gamma\left(2 - \frac{1}{2} \lambda^k(\alpha, J)\right) v_0 \sigma^k(\alpha, J, v_0) \times \left(\frac{\bar{v}}{v_0}\right)^{1-\lambda^k(\alpha, J)} \quad (46)$$

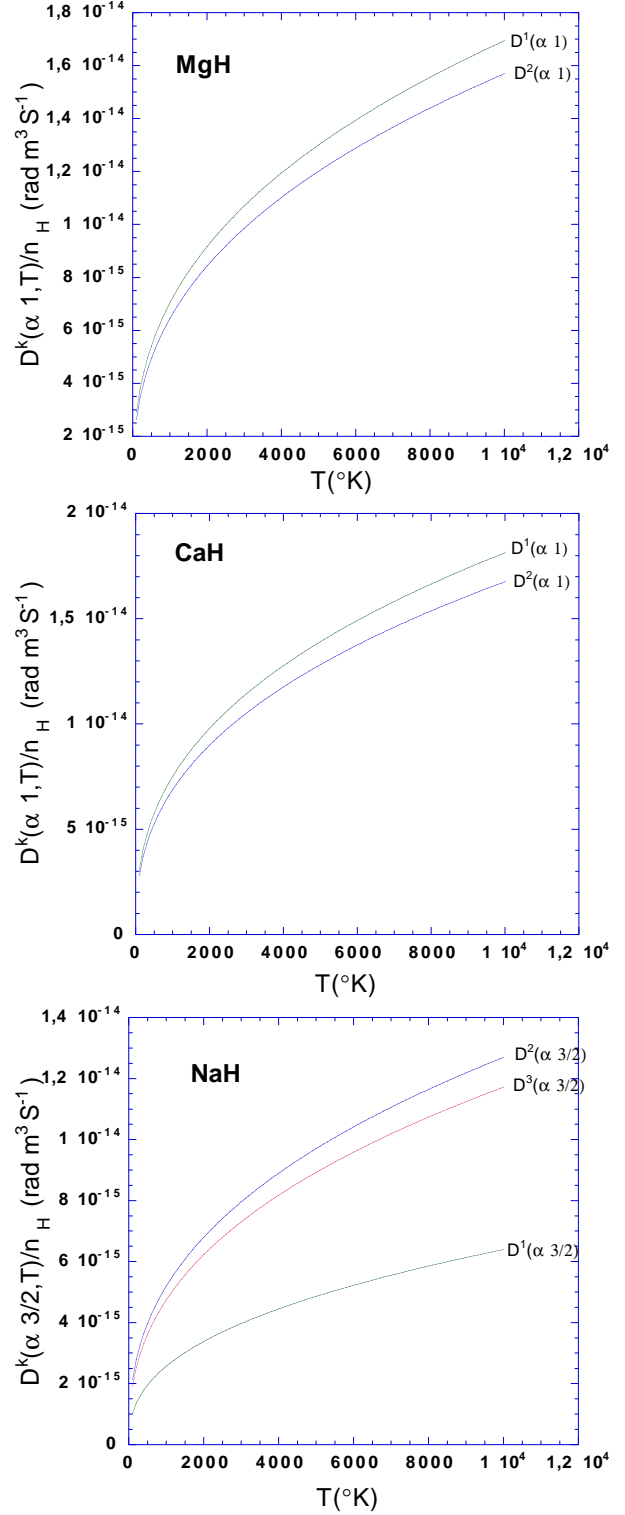


**Fig. 4.** Depolarization rates as a function of temperature.

Since  $f(v)$  depends on the reduced mass  $\mu$ , the depolarization rate is specific to a given atom. In order to obtain depolarization rates for any level of any atom by simple interpolation we applied the approximation:  $\mu = m_H, m_H$  being the hydrogen mass. We verified that this approxima-

| $n^*$ | T=5000K             |                                 | T=6000K             |                                 |
|-------|---------------------|---------------------------------|---------------------|---------------------------------|
|       | $D^2(\alpha_1)/n_H$ | $D^2(\alpha_{\frac{3}{2}})/n_H$ | $D^2(\alpha_1)/n_H$ | $D^2(\alpha_{\frac{3}{2}})/n_H$ |
| 1.5   | 0.5338              | 0.3931                          | 0.5705              | 0.4206                          |
| 1.6   | 0.6135              | 0.4477                          | 0.6556              | 0.4789                          |
| 1.7   | 0.7188              | 0.5220                          | 0.7679              | 0.5585                          |
| 1.8   | 0.8363              | 0.6047                          | 0.8944              | 0.6470                          |
| 1.9   | 0.9716              | 0.7000                          | 1.0395              | 0.7492                          |
| 2.    | 1.1260              | 0.8084                          | 1.2050              | 0.8653                          |
| 2.1   | 1.2971              | 0.9289                          | 1.3885              | 0.9944                          |
| 2.2   | 1.4844              | 1.0599                          | 1.5891              | 1.1349                          |
| 2.3   | 1.6875              | 1.2021                          | 1.8066              | 1.2872                          |
| 2.4   | 1.9043              | 1.3563                          | 2.0390              | 1.4523                          |
| 2.5   | 2.1452              | 1.5270                          | 2.2982              | 1.6352                          |
| 2.6   | 2.4065              | 1.7086                          | 2.5774              | 1.8297                          |
| 2.7   | 2.6814              | 1.9010                          | 2.8709              | 2.0348                          |
| 2.8   | 2.9634              | 2.1015                          | 3.1695              | 2.2469                          |
| 2.9   | 3.2665              | 2.3097                          | 3.5001              | 2.4707                          |
| 3.    | 3.5842              | 2.5237                          | 3.8410              | 2.6992                          |

**Table 4.** Depolarization rates for  $l = 1$ . Each column:  $S = 0$  and  $J = 1$ ;  $S = \frac{1}{2}$  and  $J = \frac{3}{2}$  for T=5000K and T=6000K, as a function of  $n^*$ . Depolarization rates are given in  $10^{-14}$  rad.  $m^3 s^{-1}$ .

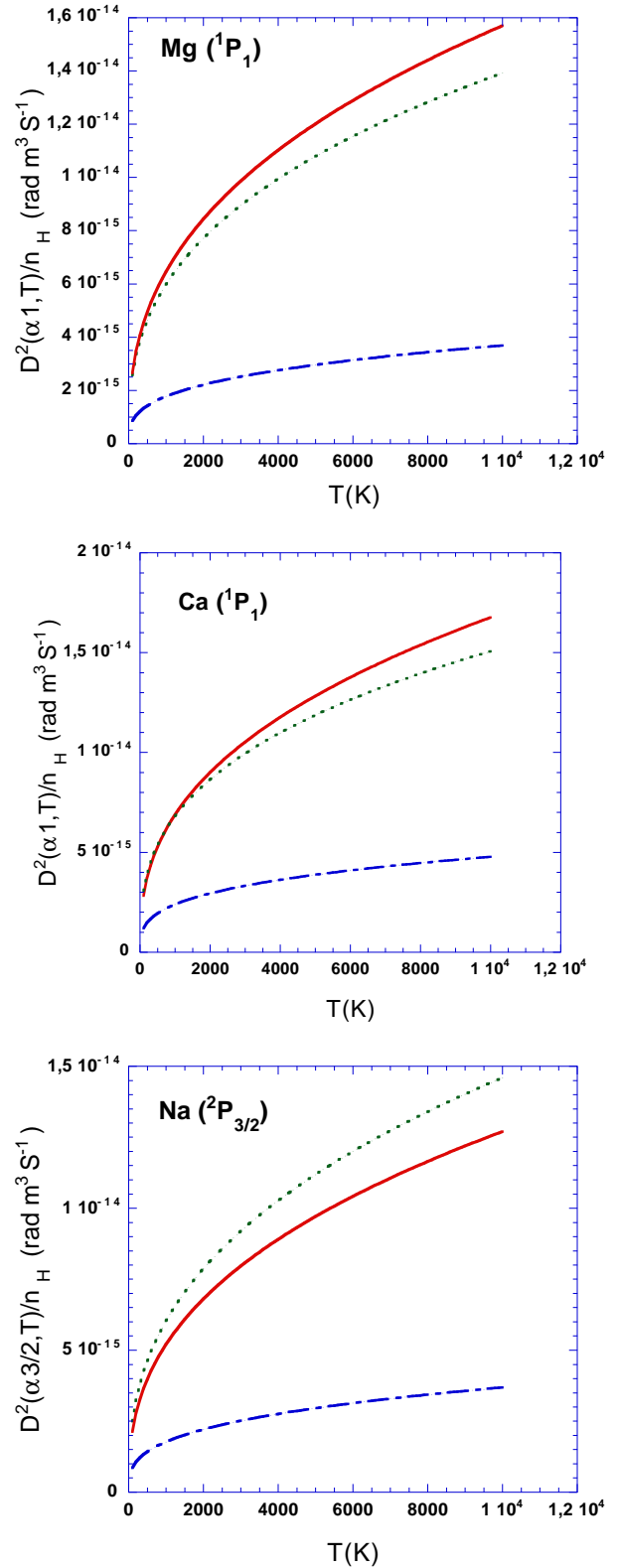
tion introduces a less than 4% error in the depolarization rates.

Table 4 gives the alignment depolarization rates as a function of  $n^*$  for the temperatures of 5000 K and 6000 K.

## 7.2. Comparison with other methods

In Figure 5 we compare our alignment depolarization rates with quantum chemistry depolarization rates (Kerkeni 2002) and the alignment depolarization rates obtained by replacing the RSU potential by the Van der Waals potential,  $V = -\frac{C_6}{R^6}$ , where  $C_6$  is the Van der Waals constant.

We display only the  $k = 2$  case which is related to the linear depolarization (alignment). Our results show rather good agreement with quantum chemistry calculations. However, the Van der Waals potential underestimates the depolarization cross section. To explain this we now examine the sensitivity of the depolarization cross section to the RSU potential.



**Fig. 5.** Depolarization rates for  $k = 2$  as a function of temperature. Full lines: our results; dotted lines: quantum chemistry calculations (Kerkeni 2002); dot-dashed lines Van der Waals approximation.

## 8. Dependence of depolarization cross sections on potentials

As a first check on the sensitivity of the results to the nature of the potential we introduce a localised perturbation to the interaction potential. We have chosen the case CaI  $4p$  for the check. The interaction potential is multiplied by a Gaussian magnification factor of the form (Anstee & O'Mara 1991)

$$G(R) = 1 + \exp(-(R - R_0)^2). \quad (47)$$

The  $\sigma$ -symmetry interaction ( $1s, 4p\sigma$ ) is more important than the  $\pi$ -symmetry interaction ( $1s, 4p\pi$ ). Therefore only the ( $1s, 4p\sigma$ ) interaction has been altered.  $R_0$  is the position of the maximum perturbation.

Fig. 6 shows the effect of the  $R_0$  variation on the depolarization cross section for three different velocities. We remark that the enhancement effect on the cross section shows a peak in the intermediate range ( $10a_0 \leq R_0 \leq 18a_0$ ). We conclude that the depolarization cross section depends most strongly on the intermediate region of the potential. It is for this reason that the Van der Waals interaction potential, which is inaccurate in this intermediate region, underestimates the depolarization cross sections.

To study the sensitivity of the cross section to close collisions, a second check is made. We have calculated the alignment cross sections by varying the cutoff  $b_0$  in equation (43). Fig. 7 shows the effect of the cutoff variation at  $v = 10 \text{ km s}^{-1}$  and  $v = 30 \text{ km s}^{-1}$ . For  $b_0 < 8a_0$  the cutoff variation does not have any effect on the cross section calculations.

Therefore it can be concluded that short-range collisions which involve ionic and exchange interactions do not influence the depolarization cross sections and hence the depolarization rates. The principal differences between the RSU potentials and those from quantum chemistry occur at small interatomic separations. Since the important impact-parameters are at medium interatomic distances, this explains why we obtain a rather good agreement between the ABO and quantum chemistry results. However, a more detailed study would be desirable but is outside the scope of the present paper because the exact quantum chemistry potentials are needed for quantitative comparison.

## 9. Conclusion

In conclusion, we have shown that the ABO theory is a powerful tool for quickly calculating a great number of depolarization cross sections for collisions with atomic hydrogen in the physical conditions of the solar atmosphere. The present paper is limited to  $p$  states for testing the method. Comparison with quantum chemistry results gives us the conviction that it would be useful to extend our calculations to higher  $l$ -values which are also of importance for solar line polarization. Although less accurate than quantum chemistry calculations, an extension to heavy atoms and higher  $l$ -values is easier and faster

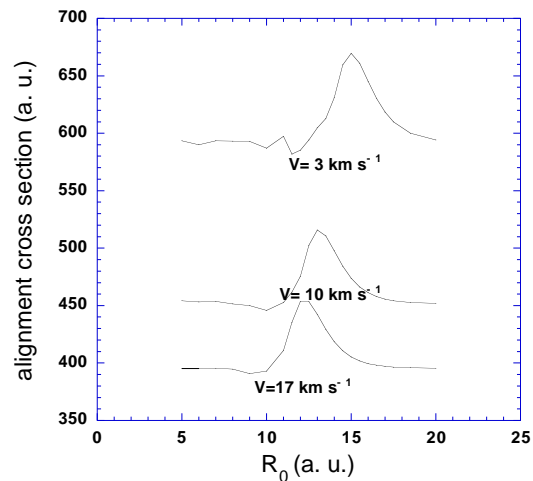


**Fig. 6.** Depolarization cross section enhancement due to a Gaussian local perturbation of the potential. Cross sections are calculated for the relative velocities:  $3 \text{ km s}^{-1}$ ,  $10 \text{ km s}^{-1}$  and  $17 \text{ km s}^{-1}$ .

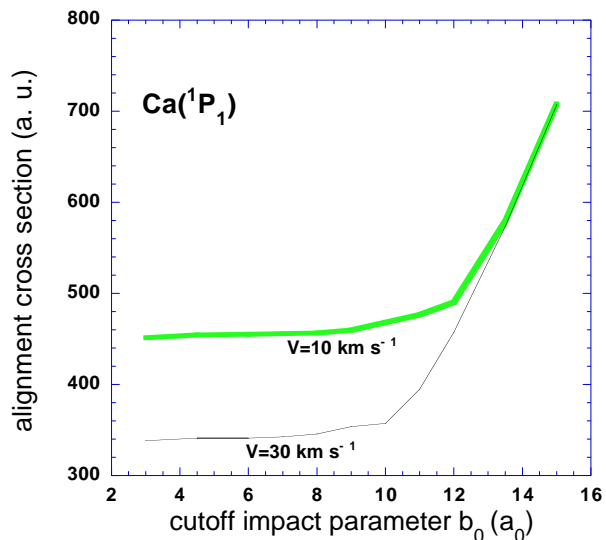


**Fig. 7.** Behaviour of the depolarization cross sections from equation (43) with the cut-off  $b_0$ . For a relative velocities  $v = 10 \text{ km s}^{-1}$  and  $v = 30 \text{ km s}^{-1}$ .

within the present semi-classical method. We will also extend our semi-classical theory to depolarization cross sections by collisions with singly ionized atoms. This will be the subject of further papers.

*Acknowledgements.* This paper is dedicated to Jim O'Mara's memory, who followed with interest the progress of the present work and suddenly passed away on April 27, 2002. The authors thank the referee for valuable suggestions which improved the presentation of this work. We are indebted to B. Kerkeni who has communicated a number of her results before publication.

## References

- Ackermann H., 1966, Colloques Internationaux du CNRS (Paris, France: editions du CNRS), N° 164, 82
- Anstee S.D., & O'Mara B.J., 1991, MNRAS, 253, 549
- Anstee S.D. PhD thesis, Univ. Queensland, 1992
- Anstee S.D., & O'Mara B.J., 1995, MNRAS, 276, 859
- Anstee S.D., O'Mara B.J., & Ross J.E., 1997, MNRAS, 284, 202
- Barklem P.S., & O'Mara B.J., 1997, MNRAS, 290, 102
- Barklem P.S., & O'Mara B.J., & Ross J.E., 1998, MNRAS, 296, 1057
- Barklem P.S. PhD thesis , Univ. Queensland, 1998
- Barklem P.S, Anstee S.D., O'Mara B.J., 1998, PASA 15(3), 336.
- Barklem P.S., Piskunov N., & O'Mara B.J., 2000, A&A, 142, 467
- Bommier V., & Sahal-Bréchet S., 1982, Solar Physics, 78, 157
- Bommier V., & Molodij G., 2002, A&A, 381, 241
- Brueckner K.A., 1971, ApJ, 169, 621
- Fano U., & Racah G., 1959, Irreducible Tensorial Sets (New York; Academic Press)
- Fano U., 1963, Phys. Rev., 131, 259
- Gangrsky Yu.P., Karaivanov D.V., Marinova K.P., Markov B.N., Melnikova L.M., Mishinsky G.V., Zemlyanoi S.G., & Zhemmenik V.I., 1998, Eur. Phys. J. A, 3, 313
- Gaupp A., Kuske P., & Andra H.J., 1982, Phys. Rev., A26, 3351
- Gordeyev E.P., Nikitin E.E., & Ovchinnikova M. Ya., 1969, Can. J. Phys., 47, 1819
- Kerkeni B., Spielfiedel A., & Feautrier N., 2000, A&A, 358, 373
- Kerkeni B., 2002, A&A, 390, 791
- Kerkeni B., & Bommier V., 2002, A&A, 394, 707
- Messiah A., 1961, Mécanique Quantique (Paris: Dunod)
- O'Mara B.J., 1976, MNRAS, 177, 551
- Omont A., 1977, Prog. Quan. Elec., 5, 69
- Roueff E., 1974, J.Phys. B, 7, 185
- Roueff E., & Suzor A., 1974, J.Phys. B, 35, 727
- Sahal-Bréchet S., 1973, A&A, 32, 147
- Sahal-Bréchet S., 1977, ApJ., 213, 887
- Seaton M.J., 1958, MNRAS, 118, 504
- Stenflo J.O., & Keller C.U., 1997, A&A, 321, 927
- Unsöld A.L., 1927, Zeitschrit für Physik, 43, 574
- Unsöld A.L., 1955, Physik der Stern Atmosphären (Zweite Auflage)
- Wiese W. L., Smith M. W., & Miles B. M., 1969, Atomic Transition Probabilities - Sodium through Calcium. U. S. Dept. of Commerce, National Bureau of Standards, Washington